CBPF-NF-018/00

Effect of nuclear deformation on the alpha-decay half-life of even-even alpha emitters†

A. Dimarco, S. B. Duarte, O. A. P. Tavares

Centro Brasileiro de Pesquisas Físicas-CBPF
Rua Dr. Xavier Sigaud 150, 22290-180 Rio de Janeiro-RJ, Brazil

M. Gonçalves

Instituto de Radioproteção e Dosimetria-IRD/CNEN
Av. Salvador Allende s/n, 22780-160 Rio de Janeiro-RJ, Brazil

F. García

Departamento de Ciências Exatas e Tecnológicas,
Universidade Estadual de Santa Cruz, 45650-000 Ilhéus-Ba, Brazil

O. Rodríguez* and F. GUZMÁN*

Instituto de Física, Universidade de São Paulo,
Caixa Postal 66318, 05315-970 São Paulo-SP, Brazil

Abstract

Alpha-decay half-life of even-even emitters has been calculated in terms of a tunnelling through a quantum mechanical potential barrier. A multipolar expansion of Coulomb potential has been developed taking into account the nuclear quadrupole, hexadecapole, and hexacontatetrapole deformations. We show that using a free-parameter model the calculated half-lives do not vary significantly with higher order multipolarities of the daughter nucleus deformation.

†Dedicated to the memory of Prof. Dr. H. G. de Carvalho.

*Permanent address: Instituto Superior de Ciencias y Tecnología Nucleares, Av. Salvador Allende y Luaces, Apartado Postal 6163, La Habana, Cuba.

1 INTRODUCTION

The alpha-decay process was interpreted in the early 1920s in terms of tunnelling through a quantum mechanical potential barrier [1, 2]. Nuclear deformation effects have been studied in 1950s by Bohr *et al* [3] and Fröman [4]. Recently, two theoretical extreme approaches have been developed to describe the alpha decay: the cluster- and fission-like theories [5]. A lot of new experimental and theoretical investigation on alpha decay half-life has been developed during the last three years or so [6-20]. An important study about alpha and beta decay for astrophysical and radioactive-ion-beam applications has been undertaken by Möller *et al* in [21]. In addition, half-life values for spontaneous nuclear decay processes (proton emission, alpha decay, cluster radioactivity, and cold fission) have been presented very recently in the framework of the Effective Liquid Drop Model [22].

On one hand, the studies mentioned above have been mainly motivated by the interest in searching for the heaviest elements, since their alpha-decay chains provide signatures of the structure of the nuclei which start the decay sequence. On the other hand, experimental efforts have been focused on the improvement of the measurement of alpha particle energies and decay half-lives as well.

The aim of this work is to take into account for nuclear deformation in order to perform alpha-decay half-life calculations. Similar purpose was pursued in Ref [18] in the study of the lifetimes for exotic radioactivities of nuclear ground-state deformations and of attenuation of fragment shell effects by the fragments' interaction.

We calculate the alpha-decay half-lives of even-even emitters for the favored alpha transitions in terms of a tunnelling through a quantum mechanical potential barrier. We developed a general expression for the deformed multipolar Coulomb potential taking into account for the quadrupole, hexadecapole, and hexacontatetrapole nuclear deformations.

In the computation of the half-life we assume that the deformed product nucleus is equivalent to a spherical one for which the barrier height is obtained by averaging the value of the potential at contact over the nuclear surface in all directions. We show that the present method of an equivalent barrier is well succeeded in reproducing the experimental data with quadrupolar deformation. It is also verified that half-life results are not affected appreciably by higher order multipolarities of the deformed daughter nucleus.

In Sec. 2 the model and calculation method are presented. Results are shown in Sec. 3. Finally, a discussion with conclusion are given in Sec. 4.

2 MODEL AND CALCULATION METHOD

The polar-angle dependence of the alpha decay rate is written as [23]:

$$\lambda(\theta) = \lambda_0(\theta) \exp\left\{ -\frac{2}{\hbar} \int_{\xi_1(\theta)}^{\xi_2(\theta)} \sqrt{2\mu\left[V(r,\theta) - Q\right]}\mathrm{d}r \right\}, \qquad (1)$$

where $\lambda_0(\theta)$ is the alpha particle frequency of assaults on the barrier, μ is the reduced mass, Q is the total kinetic energy available for the final fragments (the Q-value), $\xi_1(\theta)$

and $\xi_2(\theta)$ are the inner and outer turning points, respectively, and $V(r,\theta)$ is the Coulomb potential barrier given by

$$V(r,\theta) = \frac{Z_2 Z_\alpha e^2}{r} S(r,\theta). \tag{2}$$

In this expression Z_2 is the proton number of the daughter nucleus, $Z_\alpha = 2$, r is the distance between the centers of the alpha particle and the daughter nucleus, e is the electronic charge, and the function $S(r,\theta)$ is a multipolar expansion which describes the nuclear deformation of the product nucleus (see Appendix).

The frequency of assaults on the barrier is calculated as

$$\lambda_0(\theta) = \frac{1}{2}\sqrt{\frac{2Q}{\mu}}\frac{1}{r_2(\theta)+r_\alpha}, \tag{3}$$

where r_α =1.62 fm is the equivalent sharp charge radius of the alpha particle, and $r_2(\theta)$ is a multipolar expansion for the radius of daughter nucleus as described in the Appendix.

The inner turning point is given by

$$\xi_1(\theta) = r_2(\theta) + r_\alpha, \tag{4}$$

and the outer turning point is the root of the equation

$$V(\xi_2,\theta) - Q = 0. \tag{5}$$

In the computation of the half-life-values we assume that the deformed daughter nucleus is equivalent to a spherical one for which the potential barrier height is obtained by averaging the value of the potential at contact over the nuclear surface in all directions. Therefore, the potential barrier is given by

$$V_{eq}(r) = \frac{\overline{V}}{r/\overline{r}_2}, \tag{6}$$

where

$$\overline{V} = \frac{1}{2}\int_0^\pi V\left(r_2(\theta)+r_\alpha,\theta\right)\sin\theta \mathrm{d}\theta, \tag{7}$$

and

$$\overline{r}_2 = \frac{1}{2}\int_0^\pi r_2(\theta)\sin\theta \mathrm{d}\theta. \tag{8}$$

The decay constant is thus obtained by the expression

$$\lambda = \overline{\lambda}_0 \exp\left\{-\frac{2}{\hbar}\int_{\zeta_1}^{\zeta_2}\sqrt{2\mu\left[V_{eq}(r)-Q\right]}\mathrm{d}r\right\}, \tag{9}$$

and the alpha-decay half-life-values are given by

$$\tau_c = \frac{\ln 2}{\lambda}, \tag{10}$$

where

$$\zeta_1 = \overline{\xi}_1 = \overline{r}_2 + r_\alpha, \tag{11}$$

ζ_2 is the solution of the of equation

$$V_{eq}(\zeta_2) - Q = 0, \tag{12}$$

and

$$\overline{\lambda}_0 = \frac{1}{2}\int_0^\pi \lambda_0(\theta)\sin\theta \mathrm{d}\theta. \tag{13}$$

3 RESULTS

We have performed the present half-life calculation under the spherical approximation for the daughter nucleus as well as by taking into account for its deformation. The amount of deformation depends on the values of the multipolar expansion coefficients, α_l, as they appear in Table 1. The coefficients α_l are related to the multipolar deformation parameters, β_l, through Eq. (21) in the Appendix. The values of parameters β_l have been taken from Ref. [24].

Figure 1-a shows the expansions as defined in Table 1 for ^{248}Cm, which is the daughter nucleus in the alpha decay of ^{252}Cf. ^{248}Cm is a prolate-like nucleus because its quadrupole deformation parameter is positive ($\beta_2 = 0.235$, $\beta_4 = 0.040$, $\beta_6 = -0.036$). A graphic similar to Fig. 1-a is reported in Ref. [4]. In Figure 1-b we show $\lambda(\theta)$ for the preferred alpha decay of ^{252}Cf.

Figure 2 shows the case for alpha decay of ^{192}Pb. In Figure 2-a the radius expansions for the daughter ^{188}Hg have been depicted. In this case we have an oblate-shaped daughter nucleus because its quadrupole deformation parameter is negative ($\beta_2 = -0.130$, $\beta_4 = -0.125$, $\beta_6 = 0.001$). Figure 2-b shows the polar-angle dependence of the decay rate, $\lambda(\theta)$, for alpha decay of ^{192}Pb (ground state to ground state transitions).

In Figure 3 we show $\lambda(\theta)$ for the alpha decay of ^{206}Po. The values for the deformation parameters of the daughter nucleus ^{202}Pb are particularly small ($\beta_2 = 0.008$, $\beta_4 = -0.008$, $\beta_6 = 0.001$), therefore, leading to a somewhat different trend as compared to the precedent examples.

We define the quantities u and v as

$$u = \frac{\tau_2}{\tau}, \tag{14}$$

and

$$v = \frac{\tau_{2,4,6}}{\tau_s}, \tag{15}$$

where τ denotes the experimental alpha decay half-life, the values of which have been updated from the edition produced by the NNDC (BNL, Upton, N. Y., USA) [25], τ_s is the calculated half-life under the spherical approximation, τ_2 is the calculated half-life given by Eq. (10) by including only the nuclear quadrupole deformation, and $\tau_{2,4,6}$ represents the calculated half-life which includes the quadrupole, hexadecapole, and hexacontatetrapole

nuclear deformations. The reduced mass, μ, and the Q-value have been calculated as in Ref. [23].

A systematic study over 166 cases of preferred alpha decay of even-even parent nuclei has been undertaken by comparing calculated values with experimental ones. Table 2 shows the values for the standard deviation, σ, mean value, $\overline{q}$, ($q \equiv \log_{10}(\tau_c/\tau)$), and the number of cases rejected (i. e., those for which $|q| > 2\sigma$), n, which resulted after three runs for each gaussian-like q distribution. Here, the quantity q has been calculated for the spherical approximation, quadrupole deformation, quadrupole plus hexadecapole deformations, and quadrupole plus hexadecapole plus hexacontatetrapole deformations included.

In figure 4 we plot the ratios u (part (a)) and v (part(b)) against neutron number of the parent nucleus, N. The dashed lines indicate the region where results have been obtained within two standard deviation.

Finally, Table 3 lists and compares the calculated and experimental half-life-values for 166 cases of known preferred, ground-state to ground-state alpha decays.

4 DISCUSSION AND CONCLUSION

As we can see in Figures 1-a and 2-a, ^{248}Cm and ^{188}Hg appear to be revolution solids, where the rotation axis is the z axis. Looking at part (b) of Figs. 1 and 2 we see that the decay constant is a maximum when the curvature is also a maximum. For a prolate-shaped nucleus this maximum occurs at the poles, and for an oblate-shaped nucleus at the equator. When higher multipolarities are taken into account, the decay constant presents significant variations with the extension of the nuclear surface, however, the most important variations are given by the quadrupole deformation. These angular variations in the decay constant are not sufficient to produce important improvement on the calculated half-life, as we can see in figure 4 and Table 3. The quadrupole deformation results to be the relevant mode of deformation to be included in the calculation. When higher order multipolarities are considered, it results that their effects are indeed very small (or even negligible) as we can see in part (b) of Fig 4. This is due to the fact that deformations are indeed small, and, therefore, nuclei do not deviate appreciably from the spherical shape. The main conclusion can be drawn from the present study that the consideration of higher multipolarities to describe the nuclear shape do not lead to significant improvement in the alpha decay half-life-value by the present calculation method. We remark that after reduction of the deformed product nucleus to an average equivalent spherical one the penetrability calculation is obtained from a simplified, free-parameter Gamow-like model.

Appendix

The electrostatic potential created by a charge distribution $\rho\left(\vec{r'}\right)$at point $\vec{r}$ is given by [26]:

$$\Phi\left(\vec{r}\right) = \int\int\int_{\Omega} \frac{\rho\left(\vec{r'}\right) \mathrm{d}^3 r}{\left|\vec{r} - \vec{r'}\right|}, \tag{16}$$

where the integral is over the volume Ω occupied by the charge. If the charge distribution is independent of the position vector, we have:

$$\rho\left(\vec{r'}\right) = \frac{Z_2 e}{\Omega}, \tag{17}$$

and

$$\Phi\left(\vec{r}\right) = \frac{Z_2 e}{\Omega} \int\int\int_{\Omega} \frac{r'^2 \sin\theta' \mathrm{d}\theta' \mathrm{d}\phi' \mathrm{d}r'}{\left|\vec{r} - \vec{r'}\right|}, \tag{18}$$

where $Z_2 e$ is the total charge. If $\left|\vec{r'}\right| < \left|\vec{r}\right|$,

$$\frac{1}{\left|\vec{r} - \vec{r'}\right|} = 4\pi \sum_{\updownarrow=0}^{\infty} \sum_{m=-l}^{l} \frac{1}{2l+1} \frac{r'^l}{r^{l+1}} Y^*_{lm}(\theta', \phi') Y_{lm}(\theta, \phi), \tag{19}$$

where $r = \left|\vec{r}\right|$, $r' = \left|\vec{r'}\right|$and $Y_{lm}(\theta, \phi)$ are the spherical harmonics [26]. If $m = 0$ we have $Y_{l0}(\theta, \phi) = \sqrt{(2l+1)/(4\pi)} P_l(\cos\theta)$, with P_l being the Legendre polynomial of l-order.

We assume the following parametrization for the nuclear surface:

$$r(\theta) = \frac{r_0}{\Lambda} \left[1 + \sum_{l=0}^{\infty} \alpha_l P_l(\cos\theta) \right], \tag{20}$$

where $r_0 = R_{ch_2}$ as defined in [23], α_l's are the parameters of the multipolar expansion related to the multipole deformation parameters, β_l, by

$$\alpha_l = \sqrt{\frac{2l+1}{4\pi}} \beta_l, \tag{21}$$

and Λ is determined from the volume conservation

$$\Omega = \frac{2\pi}{3} \int_0^{\pi} r^3(\theta) \sin\theta \mathrm{d}\theta = \frac{4}{3}\pi r_0^3. \tag{22}$$

Putting the expansion given by Eq. (19) into Eq. (18), and by integrating over the volume Ω we obtain

$$\Phi\left(r,\theta\right)=\frac{Z_2\,e}{r}S(r,\theta). \tag{23}$$

The electrostatic potential energy of a charged particle of charge $Z_\alpha e$, as a function of r and θ, is thus given by

$$V(r,\theta)=\frac{Z_2 Z_\alpha e^2}{r}S(r,\theta), \tag{24}$$

where

$$S(r,\theta)=\frac{3}{2\Lambda^3}\sum_{l=0}^{\infty}a_l(r)P_l\left(\cos\theta\right), \tag{25}$$

$$a_l(r)=\frac{1}{l+3}\left(\frac{r_0}{r\Lambda}\right)^l I_l \tag{26}$$

$$I_l=\int_0^{\pi}\left[1+\sum_{l^*=0}^{\infty}\alpha_{l^*}P_{l^*}(\cos\theta)\right]^{l+3}P_l(\cos\theta')\sin\theta'\mathrm{d}\theta'. \tag{27}$$

In Eq. (23) we can see that the electrostatic potential has two factors. The first factor (Z_2e/r) is the electrostatic potential (outside the sphere) due to a spherical and uniform charge distribution, while the second one, the function $S(r,\theta)$, is the multipolar expansion taking into account for the nuclear deformation.

Acknowledgments

The authors wish to express their gratitude to the Brazilian FAPESP, FAPERJ, CNPq, and CLAF for partial support.

REFERENCES

[1] G. Gamow, *Z. Phys.* **51**, 204 (1928).

[2] E. U. Condon and R. W. Gurney, *Nature* **122**, 439 (1928).

[3] A. Bohr, P. O. Fröman, and B. R. Mottelson, *Dan. Mat. Fys. Medd.* **29**, no. 10 (1955).

[4] P. O. Fröman, *Mat. Fys. Skr. Dan. Vid. Selsk.* **1** no. 3 (1957)

[5] A. Săndulescu and W. Greiner, *Rep. Prog. Phys.* **55**, 1423 (1992).

[6] Yu. A. Lazarev *et al, Phys. Rev.* **C 54**, 620 (1996).

[7] R. D. Page, P. J. Woods, R. A. Cunningham, T. Davinson, N. J. Davis, A. N. James, K. Livingston, P. J. Sellin, and A. C. Shotter, *Phys. Rev.* **C 53**, 660 (1996).

[8] A. N. Andreyev, N. Bijnens, T. Enqvist, M. Huyse, P. Kuusiniemi, M. Leino, W. H. Trzaska, J. Uusitalo, and P. Van Duppen, *Z. Phys.* **A 358**, 63 (1997).

[9] C. F. Liang, P.Paris, R. K. Sheline, P.Alexa, and A. Gizon, *Phys. Rev* **C 54**, 2304 (1996).

[10] J. Wauters *et al, Phys. Rev.* **C 55**, 1192 (1997).

[11] C. R. Bingham *et al, Phys. Rev.* **C 54**, R20 (1996).

[12] K. S. Toth *et al, Phys. Rev.* **C 53**, 2513 (1996).

[13] T. Enqvist, P. Armbruster, K. Eskola, M. Leino, V. Ninov, W. H. Trzaska, and J. Uusitalo, Z. Phys. **A 354**, 9 (1996).

[14] K. Morita *et al, Z. Phys.* **A 352**, 7 (1995).

[15] C. F. Liang, P.Paris, A. Plochocki, E. Ruchowska, A. Gizon, D. Barnéoud, J. Genevey, G. Căta, and R. K. Sheline,*Z. Phys.* **A 354**, 153 (1996).

[16] N. Bijnens *et al, Z. Phys.* **A 356**, 3 (1996).

[17] P. Schuurmans *et al, Phys Rev. Lett* **77**, 4720 (1996).

[18] Y. -J. Shi and W. J. Swiatecki, *Nucl. Phys.* **A 464**, 205 (1987).

[19] O. A. P. Tavares, S. B. Duarte, O. Rodríguez, F. Guzmán, M Gonçalves, and F. García, *J. Phys. G: Nucl. Part. Phys* **24**, 1757 (1998).

[20] F. García, O. Rodríguez, M. Gonçalves, S. B. Duarte, O. A. P. Tavares and F. Guzmán, *J. Phys. G: Nucl. Part. Phys* (2000), in press [Pre-print CBPF Notas de Física-NF-011/00, February, 2000].

[21] P. Möller, J. R. Nix, and K.-L. Kratz, *At. Data Nucl. Data Tables* **66**, 131 (1997).

[22] S. B. Duarte, O. A. P. Tavares, F. Guzmán, A. Dimarco, F. García, O. Rodríguez, and M. Gonçalves, submitted to *At. Data Nucl. Data Tables* (2000)

[23] O. A. P. Tavares, *Il Nuovo Cimento* **110A**, 497 (1997).

[24] P. Möller, J. R. Nix, W. D. Myers, and W. J. Swiatecki, *At. Data Nucl. Data Tables* **59**, 185 (1995).

[25] Nuclear Data (NuDat) Retrieval Program, Generated at the National Nuclear Data Centre, Brookhaven National Laboratory, Upton N. Y. (USA), March 1998.

[26] J. D. Jackson, *Classical Electrodynamics* (John Wiley, N. York, 1999).

Table 1: Radius expansion for the different deformations of daughter nucleus. The parameters Λ_κ ($\kappa = 1, 2$ and 3) are found by solving Eq. (22). $r_0 = R_{n_2}$ for the calculation of the inner turning point ($\xi_1(\theta)$) and the frequency of assaults on the potential barrier ($\lambda_0(\theta)$). For the potential barrier calculation, we used $r_0 = R_{ch_2}$. Both R_{n_2}-and R_{ch_2}-values have been evaluated as described in Ref. [23].

Daughter nucleus	Radius expansion
Spherical	$r_2(\theta) = r_0$
Quadrupole	$r_2(\theta) = \frac{r_0}{\Lambda_1}\left[1 + \alpha_2 P_2(\cos\theta)\right]$
Quadrupole plus hexadecapole	$r_2(\theta) = \frac{r_0}{\Lambda_2}\left[1 + \alpha_2 P_2(\cos\theta) + \alpha_4 P_4(\cos\theta)\right]$
Quadrupole plus hexadecapole plus hexacontatetrapole	$r_2(\theta) = \frac{r_0}{\Lambda_3}\left[1 + \alpha_2 P_2(\cos\theta) + \alpha_4 P_4(\cos\theta) + \alpha_6 P_6(\cos\theta)\right]$

Table 2: Standard deviation, σ, mean value, $\overline{q}$, and number of cases rejected ($|q| > 2\sigma$), n, after three runs over 166 cases of ground-state to ground state alpha decays of even-even parent nuclei.

	Deformation			
Quantity†	Spherical	Quadrupole	Quadrupole plus hexadecapole	Quadrupole plus hexadecapole plus hexacontatretapole
$\sigma = \sqrt{\frac{1}{N}\sum_{i=1}^{N} q_i^2}$	0.290	0.295	0.295	0.295
$\overline{q} = \frac{1}{N}\sum_{i=1}^{N} q_i$	0.005	-0.003	-0.003	-0.002
n	18	17	17	17

†$q_i = \log_{10}(\tau_{c_i}/\tau_i)$, where τ_{c_i} and τ_i denote, respectively, the calculated and experimental alpha-decay half-life.

Table 3: Intercomparison between alpha-decay half-life-values calculated from the present Gamow-like model with and without product nucleus deformation included, and the experimental data for ground-state to ground-state alpha transitions of 166 even-even emitters. τ is the measured alpha-decay half-life, τ_s is the calculated value under the spherical approximation for the product nuclei; τ_2 is that value when only quadrupole deformation is included; $\tau_{2,4,6}$ is the value obtained by including all deformation parameters. $u = (\tau_2/\tau)$, $v = (\tau_{2,4,6}/\tau_s)$ (all τ-values are expressed in second).

Parent nucleus			Deformation parameters of the daugther nucleus			Calculated half-life				
Z	A	τ	β_2	β_4	β_6	τ_s	τ_2	$\tau_{2,4,6}$	u	v
52	106	0.60E-04	0.009	-0.015	-0.001	0.518E-03	0.518E-03	0.518E-03	8.637	1.000
52	108	0.43E+01	0.018	0.016	0.000	0.171E+02	0.171E+02	0.171E+02	3.973	1.001
52	110	0.62E+06	0.027	0.016	0.000	0.473E+07	0.473E+07	0.473E+07	7.632	1.000
54	112	0.32E+03	0.134	0.056	-0.004	0.192E+04	0.191E+04	0.192E+04	5.979	1.000
60	144	0.72E+23	0.000	0.000	0.000	0.268E+24	0.268E+24	0.268E+24	3.726	1.000
62	146	0.32E+16	0.000	0.000	0.000	0.702E+16	0.702E+16	0.702E+16	2.194	1.000
62	148	0.22E+24	0.000	0.000	0.000	0.655E+24	0.655E+24	0.655E+24	2.978	1.000
64	148	0.23E+10	0.000	0.000	0.000	0.472E+10	0.472E+10	0.472E+10	2.054	1.000
64	150	0.56E+14	0.000	0.000	0.000	0.125E+15	0.125E+15	0.125E+15	2.225	1.000
64	152	0.34E+22	0.161	0.059	0.006	0.867E+22	0.843E+22	0.841E+22	2.478	0.970
66	150	0.12E+04	0.000	0.000	0.001	0.208E+04	0.208E+04	0.208E+04	1.733	1.000
66	152	0.86E+07	0.000	0.000	0.000	0.206E+08	0.206E+08	0.206E+08	2.392	1.000
66	154	0.95E+14	0.161	0.050	0.007	0.115E+15	0.113E+15	0.113E+15	1.189	0.980
68	152	0.11E+02	0.000	0.000	0.000	0.200E+02	0.200E+02	0.200E+02	1.815	1.000
68	154	0.48E+05	0.000	0.000	0.000	0.671E+05	0.671E+05	0.671E+05	1.398	1.000
68	156	0.23E+11	0.153	0.041	0.009	0.606E+11	0.599E+11	0.598E+11	2.603	0.986
70	154	0.44E+00	-0.008	0.000	0.001	0.735E+00	0.735E+00	0.735E+00	1.670	1.000
70	156	0.26E+03	-0.018	0.000	0.001	0.890E+03	0.890E+03	0.890E+03	3.422	1.000

Parent nucleus			Deformation parameters of the daugther nucleus			Calculated half-life				
Z	A	τ	β_2	β_4	β_6	τ_s	τ_2	$\tau_{2,4,6}$	u	v
70	158	0.43E+07	0.143	0.040	0.010	0.408E+07	0.405E+07	0.405E+07	0.943	0.993
72	156	0.25E-01	0.000	0.000	0.000	0.314E-01	0.314E-01	0.314E-01	1.255	1.000
72	158	0.65E+01	-0.008	0.000	0.001	0.112E+02	0.112E+02	0.112E+02	1.717	1.000
72	160	0.19E+04	0.125	0.030	0.008	0.265E+04	0.264E+04	0.264E+04	1.392	0.998
72	162	0.49E+06	0.161	0.034	-0.003	0.142E+07	0.140E+07	0.140E+07	2.865	0.991
72	174	0.63E+23	0.295	-0.025	-0.020	0.956E+24	0.839E+24	0.851E+24	13.313	0.890
74	158	0.90E-03	0.008	0.000	0.001	0.228E-02	0.228E-02	0.228E-02	2.537	1.000
74	160	0.10E+00	0.035	-0.008	0.001	0.154E+00	0.154E+00	0.154E+00	1.539	1.000
74	162	0.30E+01	0.107	0.020	0.001	0.589E+01	0.589E+01	0.589E+01	1.962	1.000
74	164	0.25E+03	0.152	0.024	0.002	0.343E+03	0.342E+03	0.341E+03	1.367	0.996
74	166	0.47E+05	0.180	0.012	-0.004	0.430E+05	0.426E+05	0.425E+05	0.906	0.990
74	168	0.16E+07	0.208	0.008	-0.006	0.420E+07	0.413E+07	0.413E+07	2.583	0.982
76	162	0.19E-02	0.018	0.000	0.002	0.320E-02	0.320E-02	0.320E-02	1.687	1.000
76	164	0.42E-01	0.089	0.003	0.002	0.333E-01	0.333E-01	0.333E-01	0.793	1.001
76	166	0.27E+00	0.134	0.015	0.004	0.551E+00	0.551E+00	0.551E+00	2.041	1.000
76	168	0.45E+01	0.161	0.010	-0.001	0.904E+01	0.903E+01	0.902E+01	2.006	0.998
76	170	0.61E+02	0.181	-0.004	-0.005	0.145E+03	0.145E+03	0.145E+03	2.370	0.996
76	172	0.96E+04	0.208	0.000	-0.004	0.412E+04	0.408E+04	0.408E+04	0.425	0.990
76	174	0.22E+06	0.226	-0.006	-0.005	0.267E+06	0.262E+06	0.262E+06	1.191	0.983
76	186	0.63E+23	0.259	-0.084	0.001	0.291E+23	0.266E+23	0.279E+23	0.422	0.959
78	166	0.30E-03	0.045	-0.008	0.000	0.516E-03	0.516E-03	0.516E-03	1.721	1.001
78	170	0.60E-02	0.134	-0.002	0.000	0.278E-01	0.278E-01	0.278E-01	4.635	1.002
78	172	0.11E+00	0.162	-0.006	-0.002	0.182E+00	0.182E+00	0.183E+00	1.659	1.001
78	174	0.11E+01	0.171	-0.014	-0.003	0.195E+01	0.195E+01	0.195E+01	1.773	1.001
78	176	0.17E+02	0.190	-0.011	-0.002	0.291E+02	0.290E+02	0.290E+02	1.704	0.998
78	178	0.27E+03	0.226	-0.006	-0.005	0.638E+03	0.631E+03	0.632E+03	2.338	0.990
78	180	0.17E+05	0.246	-0.011	-0.006	0.184E+05	0.180E+05	0.181E+05	1.060	0.984
78	184	0.10E+09	0.238	-0.045	-0.004	0.835E+08	0.812E+08	0.824E+08	0.812	0.987
78	186	0.53E+10	0.239	-0.062	-0.001	0.533E+10	0.516E+10	0.528E+10	0.973	0.990
78	188	0.34E+13	0.229	-0.071	0.001	0.985E+12	0.948E+12	0.976E+12	0.279	0.991

Parent nucleus			Deformation parameters of the daugther nucleus			Calculated half-life				
Z	A	τ	β_2	β_4	β_6	τ_s	τ_2	$\tau_{2,4,6}$	u	v
78	190	0.10E+20	0.220	-0.082	0.011	0.728E+19	0.691E+19	0.719E+19	0.691	0.988
80	174	0.21E-02	0.107	-0.004	-0.001	0.114E-01	0.114E-01	0.114E-01	5.416	1.002
80	176	0.34E-01	0.126	-0.010	-0.002	0.256E-01	0.256E-01	0.256E-01	0.753	1.002
80	178	0.36E+00	0.153	-0.007	-0.003	0.386E+00	0.386E+00	0.386E+00	1.072	1.001
80	180	0.61E+01	0.171	-0.005	-0.003	0.554E+01	0.553E+01	0.553E+01	0.907	0.999
80	182	0.71E+02	0.254	0.008	-0.004	0.650E+02	0.642E+02	0.641E+02	0.904	0.986
80	184	0.28E+04	0.265	-0.007	-0.007	0.172E+04	0.169E+04	0.169E+04	0.603	0.982
80	186	0.41E+06	0.255	-0.026	-0.002	0.311E+06	0.303E+06	0.306E+06	0.739	0.983
80	188	0.53E+09	0.247	-0.044	0.000	0.188E+09	0.182E+09	0.185E+09	0.344	0.984
82	180	0.40E-02	-0.105	-0.027	0.000	0.108E-01	0.108E-01	0.108E-01	2.700	1.007
82	182	0.55E-01	-0.113	-0.026	0.000	0.399E-01	0.400E-01	0.401E-01	0.728	1.007
82	184	0.55E+00	-0.122	-0.026	0.000	0.406E+00	0.408E+00	0.409E+00	0.741	1.007
82	186	0.10E+02	-0.122	-0.018	-0.001	0.489E+01	0.491E+01	0.492E+01	0.491	1.005
82	188	0.11E+03	-0.130	-0.017	0.000	0.127E+03	0.127E+03	0.127E+03	1.156	1.005
82	190	0.80E+04	-0.130	-0.025	0.000	0.896E+04	0.898E+04	0.901E+04	1.122	1.005
82	192	0.37E+07	-0.130	-0.025	0.001	0.229E+07	0.229E+07	0.230E+07	0.618	1.004
82	194	0.99E+10	-0.130	-0.032	0.000	0.136E+10	0.136E+10	0.137E+10	0.137	1.004
82	210	0.37E+17	-0.008	0.000	0.000	0.725E+16	0.725E+16	0.725E+16	0.196	1.000
84	190	0.24E-02	0.000	-0.008	0.000	0.264E-02	0.264E-02	0.264E-02	1.102	1.000
84	192	0.34E-01	0.000	-0.008	0.001	0.244E-01	0.244E-01	0.244E-01	0.717	1.000
84	194	0.39E+00	0.000	-0.008	0.000	0.272E+00	0.272E+00	0.272E+00	0.697	1.000
84	196	0.59E+01	0.000	-0.008	0.000	0.437E+01	0.437E+01	0.437E+01	0.740	1.000
84	198	0.18E+03	0.000	-0.008	0.000	0.998E+02	0.998E+02	0.998E+02	0.554	1.000
84	200	0.62E+04	0.000	-0.008	0.000	0.220E+04	0.220E+04	0.220E+04	0.355	1.000
84	202	0.14E+06	0.000	-0.008	0.000	0.455E+05	0.455E+05	0.455E+05	0.325	1.000
84	204	0.19E+07	0.000	-0.008	0.000	0.465E+06	0.465E+06	0.465E+06	0.245	1.000
84	206	0.14E+08	0.008	-0.008	0.001	0.298E+07	0.298E+07	0.298E+07	0.213	1.000
84	208	0.91E+08	-0.008	-0.008	-0.001	0.111E+08	0.111E+08	0.111E+08	0.122	1.000
84	210	0.12E+08	-0.008	-0.008	0.000	0.906E+06	0.906E+06	0.906E+06	0.075	1.000
84	212	0.30E-06	0.000	0.000	0.000	0.213E-06	0.213E-06	0.213E-06	0.711	1.000

Parent nucleus			Deformation parameters of the daugther nucleus			Calculated half-life				
Z	A	τ	β_2	β_4	β_6	τ_s	τ_2	$\tau_{2,4,6}$	u	v
84	214	0.16E-03	0.000	0.008	0.000	0.176E-03	0.176E-03	0.176E-03	1.101	1.000
84	216	0.15E+00	0.000	0.008	0.000	0.169E+00	0.169E+00	0.170E+00	1.130	1.000
84	218	0.19E+03	0.009	0.009	0.001	0.217E+03	0.217E+03	0.217E+03	1.140	1.000
86	200	0.11E+01	0.000	0.015	0.000	0.951E+00	0.951E+00	0.951E+00	0.864	1.001
86	202	0.11E+02	0.000	-0.015	0.000	0.853E+01	0.853E+01	0.853E+01	0.775	1.001
86	204	0.10E+03	0.009	-0.015	0.000	0.627E+02	0.627E+02	0.627E+02	0.627	1.001
86	206	0.55E+03	0.009	-0.015	0.000	0.255E+03	0.255E+03	0.255E+03	0.463	1.001
86	208	0.24E+04	0.009	-0.015	0.001	0.767E+03	0.767E+03	0.768E+03	0.320	1.001
86	210	0.90E+04	-0.018	-0.008	-0.001	0.197E+04	0.197E+04	0.197E+04	0.219	1.000
86	212	0.14E+04	-0.018	-0.008	-0.001	0.189E+03	0.189E+03	0.189E+03	0.135	1.000
86	214	0.27E-06	0.000	0.008	0.000	0.240E-06	0.240E-06	0.240E-06	0.888	1.000
86	216	0.45E-04	0.000	0.008	0.000	0.840E-04	0.840E-04	0.840E-04	1.866	1.000
86	218	0.35E-01	-0.008	0.008	0.000	0.617E-01	0.617E-01	0.617E-01	1.764	1.000
86	220	0.56E+02	0.020	0.018	0.004	0.985E+02	0.985E+02	0.985E+02	1.758	1.001
86	222	0.33E+06	0.039	0.028	0.007	0.540E+06	0.540E+06	0.541E+06	1.636	1.002
88	202	0.70E-03	-0.215	0.002	0.000	0.300E-02	0.307E-02	0.307E-02	4.381	1.020
88	204	0.59E-01	-0.207	-0.007	0.000	0.509E-01	0.518E-01	0.518E-01	0.877	1.018
88	206	0.24E+00	-0.104	0.004	0.004	0.244E+00	0.245E+00	0.245E+00	1.022	1.003
88	208	0.14E+01	-0.087	0.003	0.004	0.718E+00	0.720E+00	0.720E+00	0.514	1.002
88	210	0.38E+01	-0.044	-0.007	-0.001	0.147E+01	0.147E+01	0.147E+01	0.387	1.001
88	212	0.14E+02	-0.026	-0.008	-0.002	0.414E+01	0.414E+01	0.414E+01	0.296	1.000
88	214	0.25E+01	-0.026	-0.008	-0.002	0.499E+00	0.499E+00	0.499E+00	0.200	1.000
88	216	0.18E-06	0.000	0.008	0.000	0.200E-06	0.200E-06	0.200E-06	1.110	1.000
88	218	0.26E-04	0.008	0.008	0.000	0.481E-04	0.481E-04	0.481E-04	1.848	1.000
88	220	0.18E-01	0.008	0.008	0.001	0.293E-01	0.293E-01	0.293E-01	1.629	1.000
88	222	0.39E+02	0.040	0.029	0.007	0.556E+02	0.556E+02	0.557E+02	1.425	1.002
88	224	0.33E+06	0.111	0.081	0.007	0.484E+06	0.483E+06	0.488E+06	1.464	1.008
88	226	0.53E+11	0.137	0.100	0.006	0.800E+11	0.792E+11	0.801E+11	1.494	1.002
90	210	0.90E-02	-0.130	-0.002	0.007	0.112E-01	0.113E-01	0.113E-01	1.254	1.007
90	212	0.30E-01	-0.104	0.004	0.008	0.203E-01	0.204E-01	0.204E-01	0.680	1.004

Parent nucleus			Deformation parameters of the daugther nucleus			Calculated half-life				
Z	A	τ	β_2	β_4	β_6	τ_s	τ_2	$\tau_{2,4,6}$	u	v
90	214	0.10E+00	-0.053	-0.007	-0.002	0.478E-01	0.479E-01	0.479E-01	0.479	1.001
90	216	0.28E-01	-0.035	-0.015	-0.003	0.724E-02	0.724E-02	0.724E-02	0.259	1.001
90	218	0.11E-06	0.008	0.008	0.000	0.162E-06	0.162E-06	0.162E-06	1.472	1.000
90	220	0.97E-05	0.008	0.008	0.001	0.198E-04	0.198E-04	0.198E-04	2.046	1.000
90	222	0.28E-02	0.020	0.010	0.003	0.351E-02	0.351E-02	0.351E-02	1.254	1.000
90	224	0.13E+01	0.103	0.072	0.007	0.159E+01	0.160E+01	0.161E+01	1.228	1.010
90	226	0.24E+04	0.130	0.092	0.008	0.323E+04	0.322E+04	0.326E+04	1.343	1.010
90	228	0.83E+08	0.164	0.112	0.010	0.107E+09	0.105E+09	0.107E+09	1.271	0.999
90	230	0.31E+13	0.172	0.112	0.007	0.418E+13	0.410E+13	0.412E+13	1.321	0.987
90	232	0.57E+18	0.180	0.113	0.005	0.858E+18	0.831E+18	0.832E+18	1.457	0.971
92	218	0.15E-02	-0.052	-0.022	-0.005	0.333E-03	0.334E-03	0.334E-03	0.223	1.003
92	222	0.10E-05	0.008	0.008	0.001	0.402E-05	0.402E-05	0.402E-05	4.017	1.000
92	224	0.90E-03	0.030	0.019	0.005	0.676E-03	0.676E-03	0.677E-03	0.751	1.001
92	226	0.20E+00	0.111	0.081	0.006	0.369E+00	0.370E+00	0.374E+00	1.849	1.012
92	230	0.27E+07	0.173	0.111	0.034	0.320E+07	0.317E+07	0.319E+07	1.175	0.996
92	232	0.32E+10	0.182	0.112	0.025	0.374E+10	0.367E+10	0.368E+10	1.148	0.986
92	234	0.11E+14	0.198	0.115	0.014	0.110E+14	0.107E+14	0.107E+14	0.976	0.969
92	236	0.10E+16	0.207	0.108	0.003	0.118E+16	0.113E+16	0.113E+16	1.135	0.958
92	238	0.18E+18	0.215	0.102	-0.007	0.269E+18	0.257E+18	0.255E+18	1.426	0.947
94	228	0.20E+00	0.146	0.100	0.006	0.336E+00	0.337E+00	0.341E+00	1.684	1.014
94	232	0.16E+05	0.191	0.114	0.029	0.114E+05	0.113E+05	0.114E+05	0.709	0.995
94	234	0.53E+06	0.199	0.115	0.020	0.682E+06	0.673E+06	0.674E+06	1.271	0.988
94	236	0.13E+09	0.207	0.117	0.010	0.980E+08	0.961E+08	0.960E+08	0.739	0.979
94	238	0.39E+10	0.215	0.110	0.000	0.275E+10	0.268E+10	0.267E+10	0.687	0.971
94	240	0.28E+12	0.215	0.102	-0.008	0.251E+12	0.243E+12	0.242E+12	0.867	0.966
94	242	0.15E+14	0.215	0.093	-0.015	0.133E+14	0.128E+14	0.128E+14	0.856	0.961
94	244	0.32E+16	0.224	0.079	-0.023	0.221E+16	0.211E+16	0.210E+16	0.658	0.950
96	240	0.33E+07	0.215	0.110	-0.004	0.172E+07	0.169E+07	0.169E+07	0.512	0.983
96	242	0.19E+08	0.215	0.102	-0.012	0.115E+08	0.113E+08	0.113E+08	0.593	0.981
96	244	0.75E+09	0.223	0.087	-0.021	0.418E+09	0.407E+09	0.407E+09	0.543	0.973

Parent nucleus			Deformation parameters of the daugther nucleus			Calculated half-life				
Z	A	τ	β_2	β_4	β_6	τ_s	τ_2	$\tau_{2,4,6}$	u	v
96	246	0.18E+12	0.224	0.071	-0.025	0.991E+11	0.959E+11	0.956E+11	0.533	0.965
96	248	0.14E+14	0.224	0.062	-0.027	0.822E+13	0.791E+13	0.788E+13	0.565	0.959
96	250	0.28E+13	0.235	0.040	-0.033	0.648E+13	0.621E+13	0.620E+13	2.217	0.956
98	240	0.64E+02	0.215	0.102	-0.002	0.470E+02	0.468E+02	0.468E+02	0.731	0.995
98	242	0.26E+03	0.215	0.093	-0.009	0.226E+03	0.224E+03	0.224E+03	0.862	0.993
98	244	0.15E+04	0.224	0.087	-0.018	0.114E+04	0.113E+04	0.113E+04	0.755	0.990
98	246	0.16E+06	0.224	0.079	-0.024	0.845E+05	0.832E+05	0.832E+05	0.520	0.985
98	248	0.35E+08	0.234	0.073	-0.029	0.149E+08	0.145E+08	0.145E+08	0.416	0.974
98	250	0.49E+09	0.234	0.057	-0.032	0.196E+09	0.190E+09	0.190E+09	0.388	0.971
98	252	0.10E+09	0.235	0.040	-0.036	0.616E+08	0.600E+08	0.600E+08	0.600	0.974
98	254	0.20E+10	0.225	0.030	-0.029	0.180E+10	0.175E+10	0.175E+10	0.874	0.971
98	256	0.74E+11	0.226	0.012	-0.024	0.216E+12	0.209E+12	0.209E+12	2.818	0.966
100	246	0.12E+01	0.224	0.079	-0.023	0.148E+01	0.148E+01	0.148E+01	1.230	0.999
100	248	0.45E+02	0.234	0.073	-0.031	0.216E+02	0.214E+02	0.215E+02	0.477	0.995
100	252	0.11E+06	0.235	0.040	-0.035	0.281E+05	0.277E+05	0.277E+05	0.252	0.984
100	254	0.14E+05	0.245	0.026	-0.041	0.605E+04	0.596E+04	0.597E+04	0.425	0.986
100	256	0.14E+06	0.236	0.015	-0.035	0.768E+05	0.755E+05	0.756E+05	0.539	0.984
102	250	0.50E+00	0.234	0.057	-0.036	0.105E+00	0.105E+00	0.105E+00	0.210	1.003
102	252	0.42E+01	0.235	0.049	-0.038	0.165E+01	0.164E+01	0.165E+01	0.391	0.999
102	254	0.72E+02	0.235	0.033	-0.040	0.174E+02	0.173E+02	0.173E+02	0.240	0.997
102	256	0.36E+01	0.245	0.018	-0.045	0.106E+01	0.105E+01	0.106E+01	0.293	1.002
102	258	0.12E+03	0.237	0.008	-0.039	0.260E+02	0.258E+02	0.259E+02	0.215	0.998
104	254	0.17E+00	0.235	0.032	-0.035	0.269E-01	0.269E-01	0.270E-01	0.159	1.004
104	256	0.36E+00	0.236	0.024	-0.038	0.432E+00	0.432E+00	0.433E+00	1.199	1.002
104	258	0.11E+00	0.246	0.011	-0.043	0.315E-01	0.315E-01	0.317E-01	0.287	1.007
104	260	0.10E+01	0.237	-0.001	-0.036	0.518E+00	0.518E+00	0.520E+00	0.518	1.003
106	260	0.85E-02	0.247	-0.007	-0.043	0.322E-02	0.324E-02	0.326E-02	0.381	1.013
108	264	0.10E-03	0.239	-0.025	-0.034	0.284E-03	0.286E-03	0.289E-03	2.862	1.018

FIGURE CAPTION

Fig. 1 The decay $^{252}\mathrm{Cf} \longrightarrow {}^{248}\mathrm{Cm} + {}^{4}\mathrm{He}$. (a) Different shapes for $^{248}\mathrm{Cm}$. (b) Angular dependence of the decay constant. The solid line denotes the case for spherical approximation, the short-dashed line that for quadrupole deformation, the dotted line refers to quadrupole plus hexadecapole deformations, and the dash-dotted line represents quadrupole plus hexadecapole plus hexacontatetrapole deformations.

Fig. 2 The same as in Fig. 1 for the decay $^{192}\mathrm{Pb} \longrightarrow {}^{188}\mathrm{Hg} + {}^{4}\mathrm{He}$.

Fig. 3 Polar-angle dependence of the decay constant for $^{206}\mathrm{Po}$ alpha decay. The notation is the same as in Fig. 1.

Fig. 4 The quantities $u = \tau_2/\tau$ (part(a)) and $v = \tau_{2,4,6}/\tau_s$ (part(b)) in $\log_{10}$-scale plotted against neutron number of the parent nucleus, N. Points represent the values of the ratios u and v for each decay case. The dashed lines define the range limited by two standard deviation.

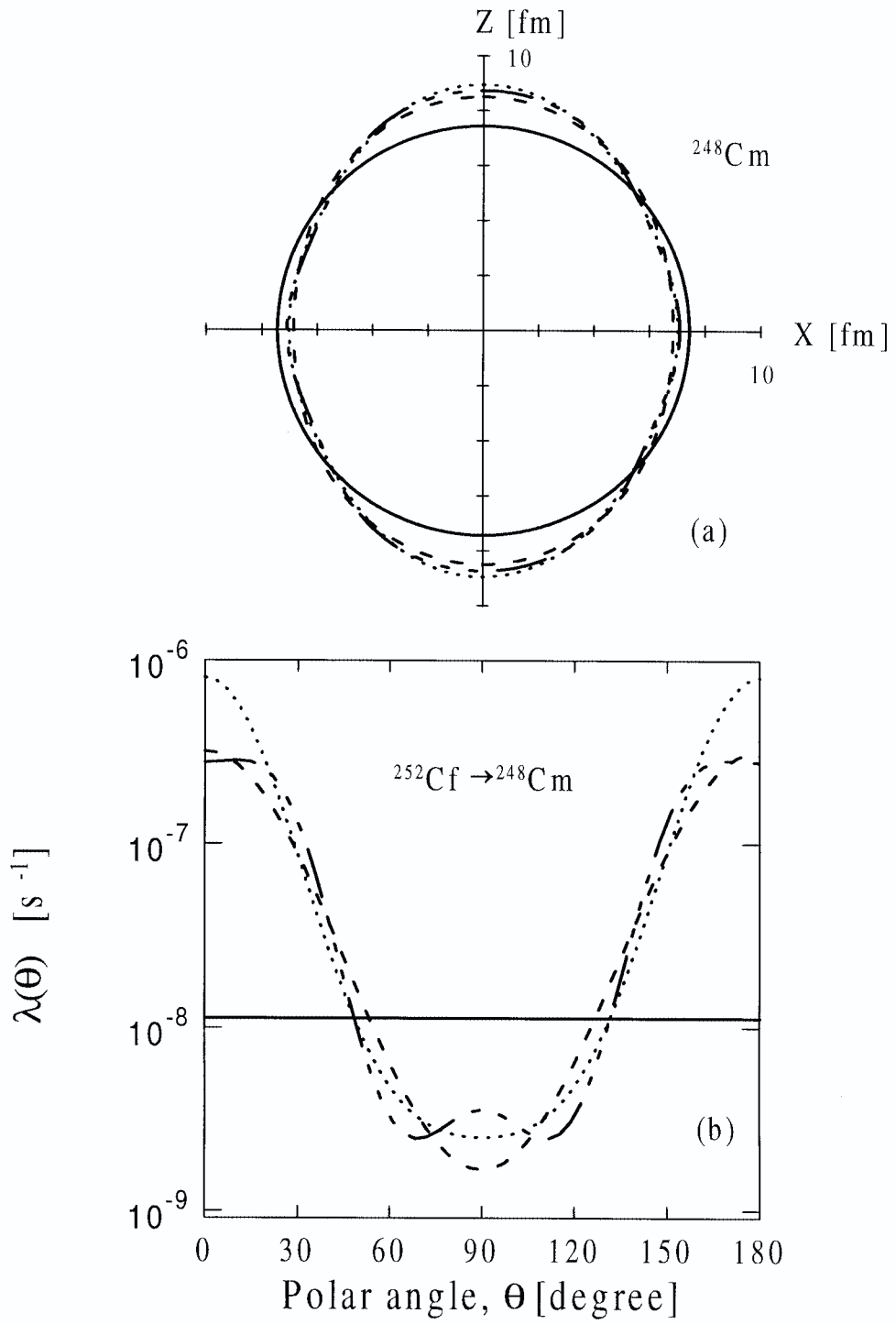

A. Dimarco, et al.
Effect of nuclear deformation on the alpha-decay half-life of even-even alpha emitters
Fig. 1

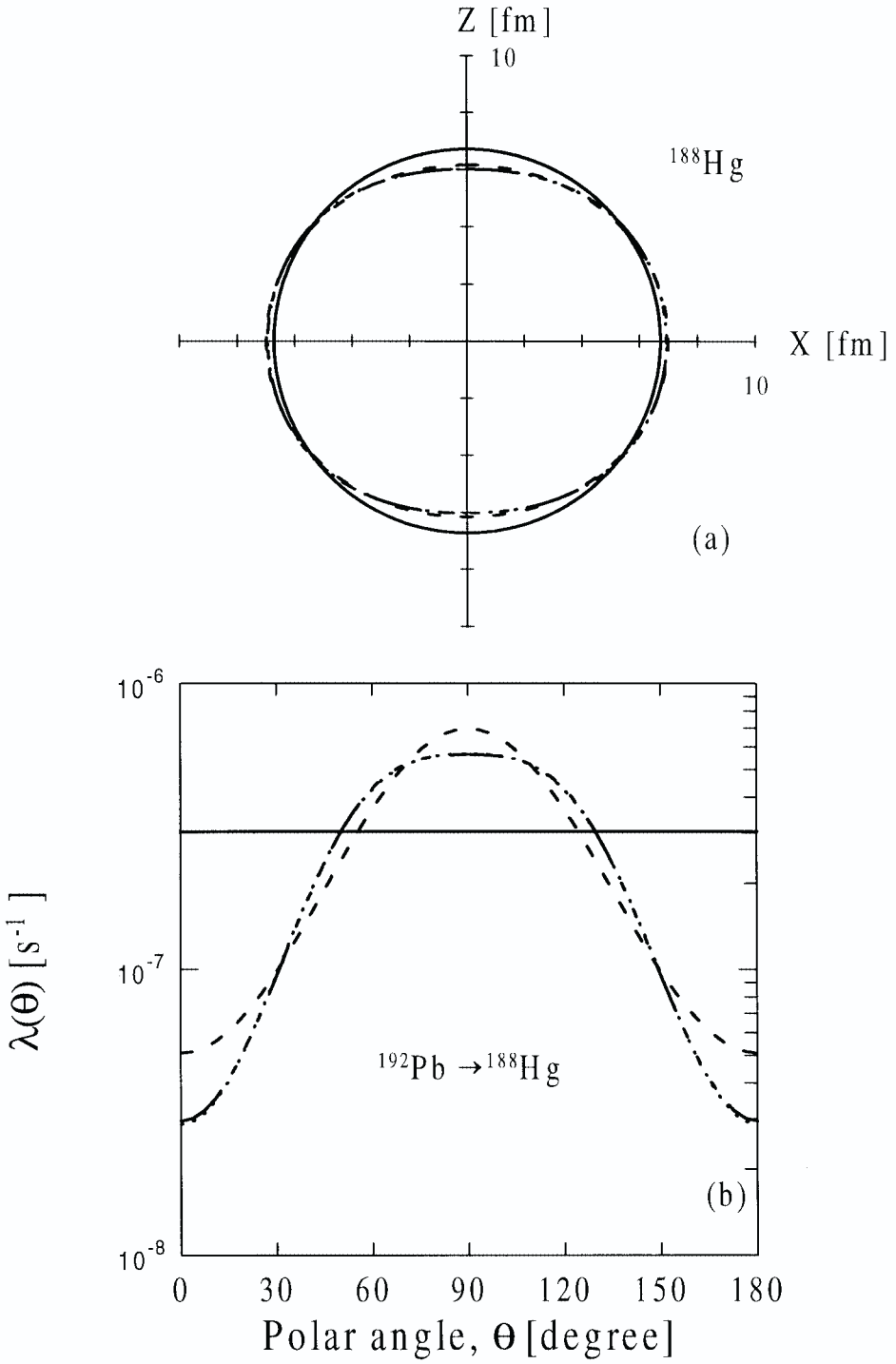

A. Dimarco, et al
Effect of nuclear deformation on the alpha-decay half-life of even-even alpha emitters
Fig. 2

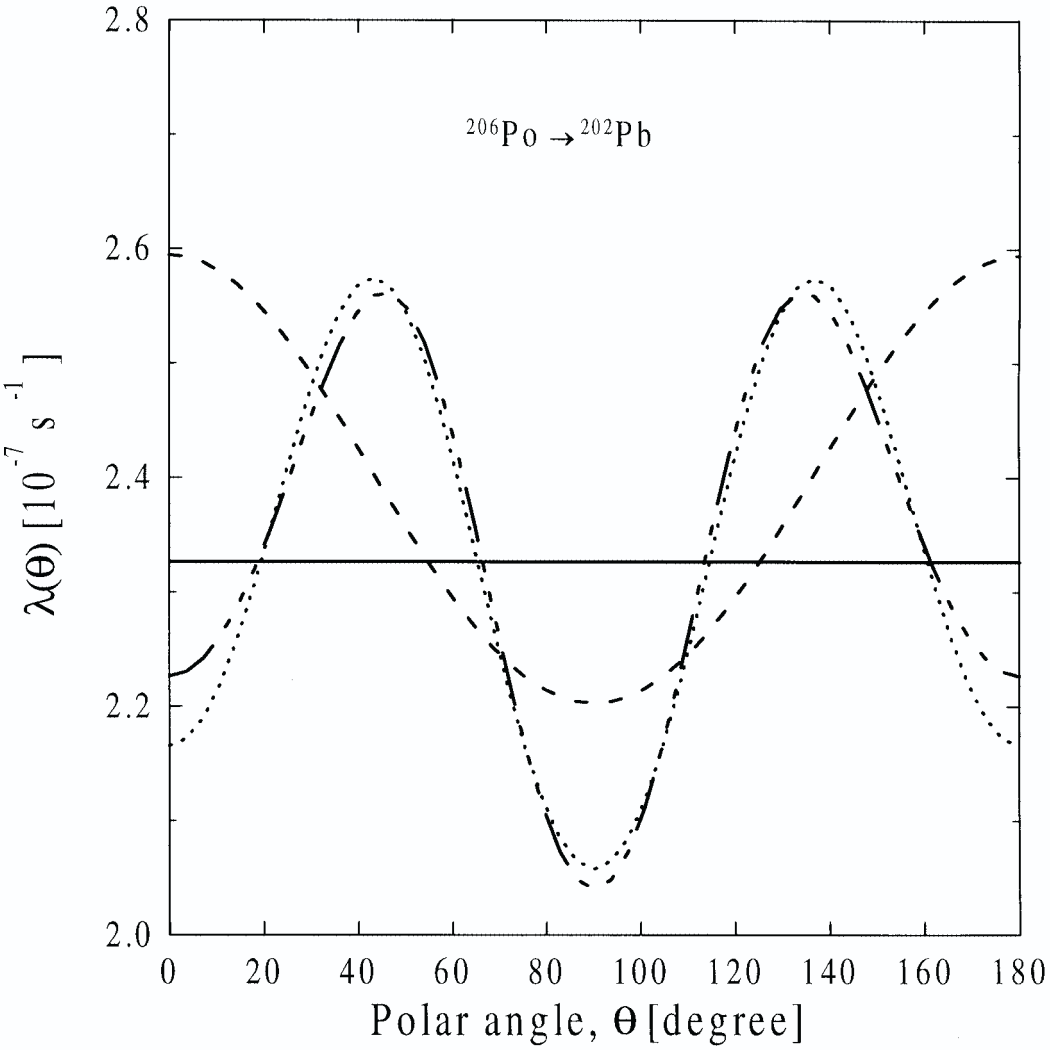

A. Dimarco, et al.
Effect of nuclear deformation on the alpha-decay half-life of even-even alpha emitters
Fig. 3

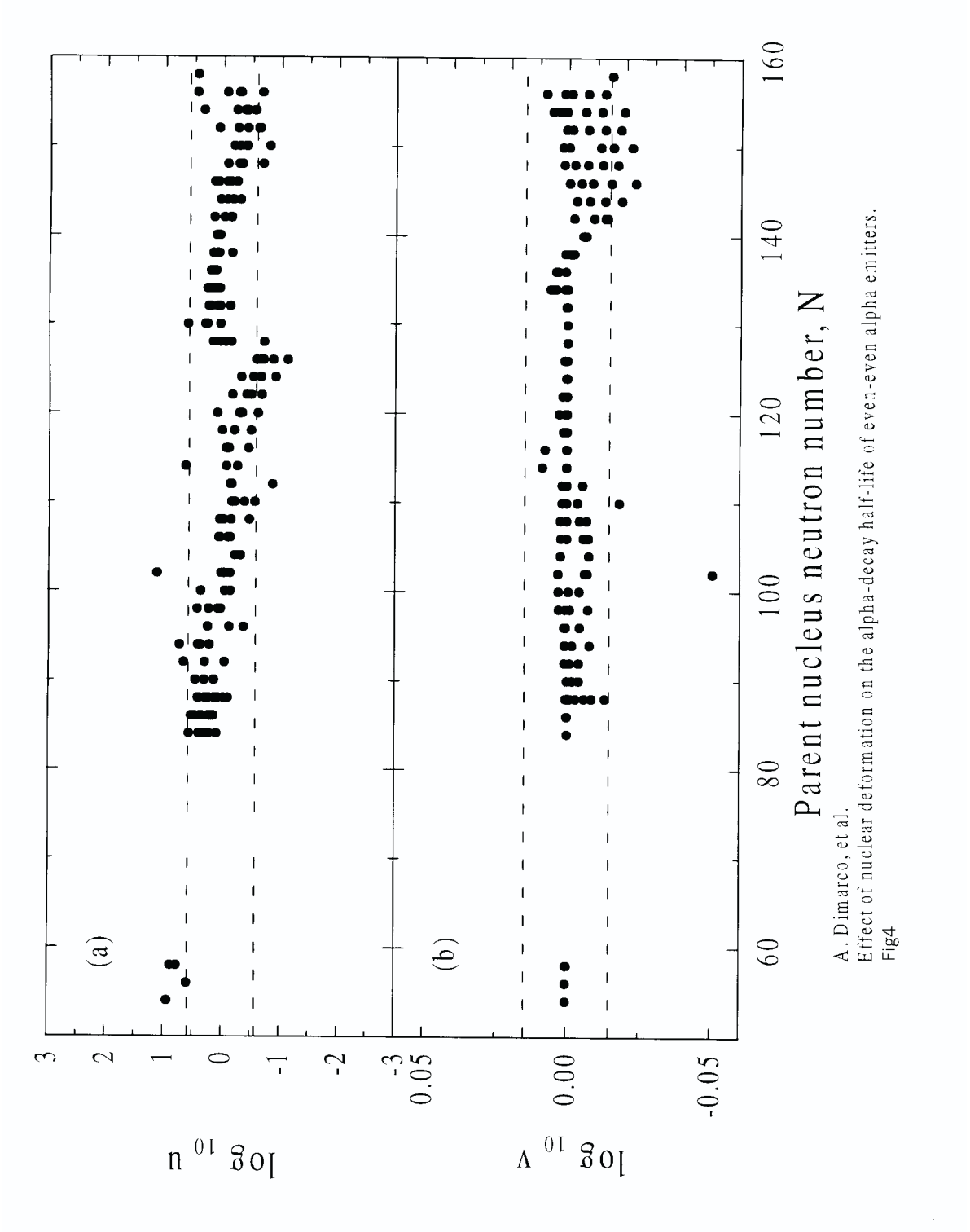

A. Dimarco, et al.
Effect of nuclear deformation on the alpha-decay half-life of even-even alpha emitters.
Fig4